Increased glymphatic influx is correlated with high EEG delta power and low heart rate in mice under anesthesia

Hablitz, Lauren M.; Vinitsky, Hanna S.; Sun, Qian; Stæger, Frederik Filip; Sigurdsson, Bjørn; Mortensen, Kristian N.; Lilius, Tuomas O.; Nedergaard, Maiken

Published in:
Science Advances

DOI:
10.1126/sciadv.aav5447

Publication date:
2019

Document version
Publisher's PDF, also known as Version of record

NEUROPHYSIOLOGY

Increased glymphatic influx is correlated with high EEG delta power and low heart rate in mice under anesthesia

Lauren M. Hablitz[1], Hanna S. Vinitsky[1], Qian Sun[1], Frederik Filip Stæger[2], Björn Sigurdsson[2], Kristian N. Mortensen[2], Tuomas O. Lilius[2,3], Maiken Nedergaard[1,2]*

The glymphatic system is responsible for brain-wide delivery of nutrients and clearance of waste via influx of cerebrospinal fluid (CSF) alongside perivascular spaces and through the brain. Glymphatic system activity increases during sleep or ketamine/xylazine (K/X) anesthesia, yet the mechanism(s) facilitating CSF influx are poorly understood. Here, we correlated influx of a CSF tracer into the brain with electroencephalogram (EEG) power, heart rate, blood pressure, and respiratory rate in wild-type mice under six different anesthesia regimens. We found that glymphatic CSF tracer influx was highest under K/X followed by isoflurane (ISO) supplemented with dexmedetomidine and pentobarbital. Mice anesthetized with α-chloralose, Avertin, or ISO exhibited low CSF tracer influx. This is the first study to show that glymphatic influx correlates positively with cortical delta power in EEG recordings and negatively with beta power and heart rate.

INTRODUCTION

Cerebrospinal fluid (CSF) can move along perivascular spaces in the brain and spinal cord to distribute nutrients and clear waste (*1*, *2*). These processes are supported by the water channel aquaporin 4 (AQP4), which is present at high density on the vascular end feet of astrocytes (*2*–*4*). CSF tracer influx to the brain is higher in animals in the sleeping than in the awake condition (*5*). Previous studies of glymphatic function have shown that anesthesia with ketamine/xylazine (K/X) emulates sleep in that fluorescent CSF tracer influx and that the rate of radiolabeled Aβ efflux from the brain is comparable to findings in naturally sleeping animals (*6*). Although it remains largely unknown whether anesthetics other than K/X influence fluid movement from the CSF compartment into the brain, one experimental magnetic resonance imaging study showed that anesthesia with isoflurane (ISO) combined with the α_2-agonist dexmedetomidine (dex) facilitated glymphatic transport of a contrast agent compared to ISO alone (*7*). The scarcity of information concerning the physiological mechanisms behind CSF transport has emerged as a limitation for current models and may contribute to controversy about the importance of AQP4 as a driver for fluid flow in the glymphatic system (*3*, *8*).

Slow cortical network oscillations (delta waves) may contribute to the efficiency of fluid influx into the brain parenchyma and clearance of waste from the brain (*5*, *9*). Delta waves are increased in naturally sleeping animals, potentially due to long-term homeostatic changes in the neuromodulatory, metabolic, and neurochemical environment (*10*) and broad synaptic scaling (*11*). Some types of sedatives, such as the α_2-adrenergic agonists xylazine and dex, induce a sharp increase in electroencephalogram (EEG) delta power, whereas anesthesia with the volatile anesthetic, ISO, or the injectable γ-aminobutyric acid type A ($GABA_A$) agonist pentobarbital maintain more high-frequency components (*7*, *12*). In addition to neuronal network oscillations, cardiopulmonary parameters such as blood pressure, heart rate, and respiratory rate can also regulate glymphatic influx, and these parameters are themselves modified by different anesthetics in drug- and dose-specific manners (*13*, *14*). Thus, anesthesia may be used to manipulate both EEG spectra and cardiopulmonary function and differentially regulate glymphatic influx. To test this hypothesis, we systematically compared glymphatic influx in mice under anesthesia with six anesthetic regimens. Groups of mice were anesthetized with K/X, pentobarbital, Avertin (2,2,2-tribromoethanol), α-chloralose, ISO supplemented with dex, and ISO alone. To establish how neural activity in conjunction with altered cardiopulmonary function controlled glymphatic influx, we recorded EEG and cardiopulmonary parameters in a separate cohort of mice under the same anesthetic conditions. Our analysis demonstrates that glymphatic influx occurs in direct proportion to the power of cortical delta wave activity, in inverse proportion to heart rate, and was most pronounced under K/X anesthesia.

RESULTS

Anesthesia alters spatial distribution of CSF tracer

We investigated how a broad range of anesthesia types influences the movement of CSF tracer from the subarachnoid space into the perivascular spaces of the brain and ultimately into the parenchyma. A previous analysis has shown that tracers injected into the rodent cisterna magna (CM) quickly distribute to the base of the brain and into the perivascular space of the circle of Willis (*1*). To visualize the perivascular space of the circle of Willis and the major cerebral arteries, including the middle cerebral artery, we first analyzed fluorescence tracer distribution at the base (ventral) and top (dorsal) surfaces of brains harvested under different anesthetic conditions. In all experiments, the tracer (bovine serum albumin, Alexa Fluor 647 conjugate; 66 kDa) was injected into the CM and allowed to distribute for 30 min before brain collection. As in our previous studies, tracer signal was higher on the ventral than on the dorsal aspect of the brain (Fig. 1). Tracer distribution was highest, as measured by

[1]Center for Translational Neuromedicine, University of Rochester Medical Center, Rochester, NY 14642, USA. [2]Center for Translational Neuromedicine, Faculty of Health and Medical Sciences, University of Copenhagen, 2200 Copenhagen, Denmark. [3]Department of Clinical Pharmacology, University of Helsinki and Helsinki University Hospital, Helsinki, Finland.
*Corresponding author. Email: nedergaard@urmc.rochester.edu

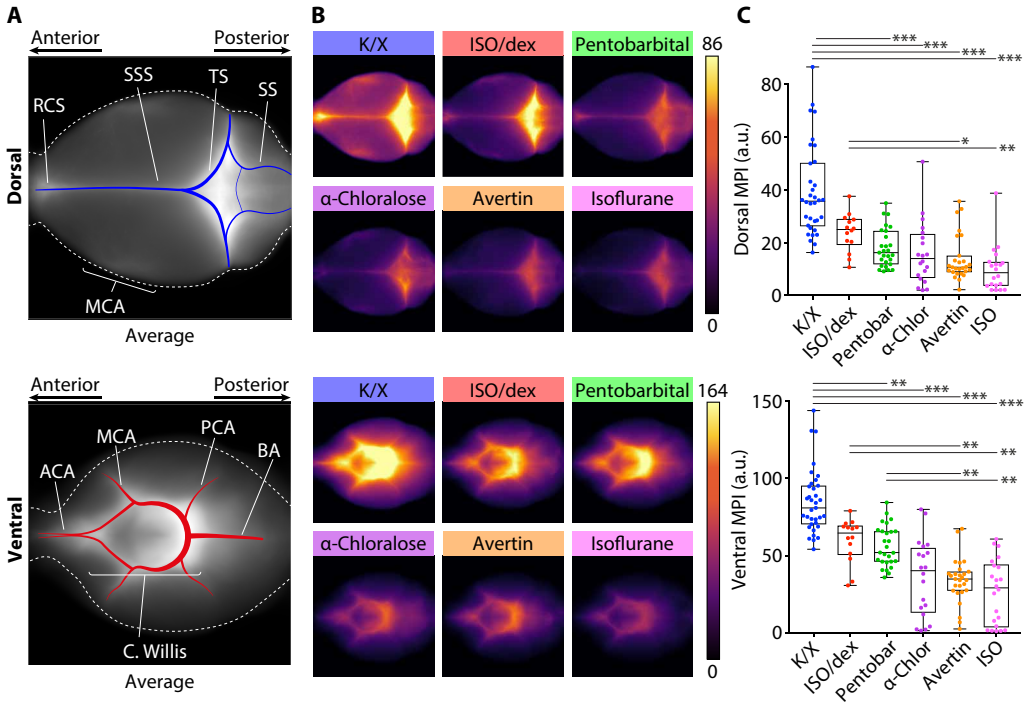

Fig. 1. Anesthetic regimen effects CSF tracer distribution at the dorsal and ventral brain surfaces. (**A**) Population-based average of tracer distribution at the dorsal (top) and ventral (bottom) brain surfaces with anatomical references. (**B**) Comparison of average tracer distribution at the dorsal (top) and ventral (bottom) brain surfaces in the six groups of anesthetized mice. (**C**) Boxplots comparing dorsal (top) and ventral (bottom) tracer distributions for the six different anesthetic agents or combinations (whiskers, minimum and maximum; box, quartiles; and line, median). Kruskal-Wallis test followed by Bonferroni correction, $^{*}P < 0.05$, $^{**}P < 0.01$, $^{***}P < 0.001$. K/X, $n = 35$ animals; ISO supplemented with dex (ISO/dex), $n = 14$ animals; pentobarbital (Pentobar), $n = 27$ animals; α-chloralose (α-chlor), $n = 20$ animals; tribromoethanol (Avertin), $n = 27$ animals; and ISO, $n = 20$ animals. ACA, anterior cerebral artery; BA, basilar artery; C. Willis, circle of Willis; ICA, internal carotid artery; MCA, middle cerebral artery; PCA, posterior cerebral artery; RCS, rostral confluence of sinuses; SS, sigmoid sinus; SSS, superior sagittal sinus; and TS, transverse sinus. a.u., arbitrary units.

mean pixel intensity (MPI) across the region of interest (ROI), under K/X anesthesia both on the dorsal (Fig. 1C and table S1) and ventral sides (Fig. 1C and table S1). Mice under ISO anesthesia supplemented with dex also displayed pronounced distribution of the tracer on the ventral and dorsal aspects of the brain, in agreement with previous findings (*7*). Pentobarbital exhibited intermediate CSF labeling on the ventral and dorsal brain surfaces. In contrast, mice anesthetized with Avertin, α-chloralose, and ISO alone all displayed poor tracer dispersion, especially on the ventral side of the brain, compared to the other anesthesia regimens.

We next prepared 100-μm-thick coronal sections through the brains and quantified the mean pixel fluorescence intensity across six slices collected at 600-μm intervals starting at 1.1 mm anterior to the bregma to calculate the mean total tracer influx per entire brain (Fig. 2and fig. S1). This analysis showed results concurring closely with the dorsal and ventral analyses, with the K/X-anesthetized mice exhibiting significantly higher influx (Fig. 2, A and B, and table S1). Supplementing ISO with dex also significantly increased the MPI compared to the ISO alone group, whereas MPI in brain slices were low in mice anesthetized with Avertin, α-chloralose, or ISO alone. Next, we tested whether tracer distribution under anesthesia varied according to brain region. A subregion analysis of ventral cortex, lateral cortex, dorsal cortex, hippocampus, thalamus, and hypothalamus revealed a similar pattern of tracer fluorescence as the averaged coronal sections across anesthetic groups (fig. S2 and table S1). Furthermore, to ensure that our signal is driven by tracer entering along the perivascular space and into the parenchyma, as compared to reflux into the ventricles or in the remaining arachnoid space of the extracted brain, we measured fluorescence specifically in the interior cortex and striatum (fig. S3). As with both the coronal section average and the subregion analysis, K/X had increased influx compared to the other anesthetic regimens in the interior brain.

We then compared dorsal and ventral fluorescent values to average slice fluorescence for each animal and conducted linear regression analysis between individual slice MPI and dorsal/ventral tracer intensity, respectively. This analysis showed a slightly better correlation between ventral tracer distributions than dorsal tracer distributions with total slice MPI ($R^2 = 0.871$ versus 0.817, $P < 0.0001$ in both cases) (Fig. 2, C and D). We saw similar significant linear regressions between the interior slice analysis and dorsal, ventral, and total slice MPIs (fig. S3), thus demonstrating that tracer distribution along the ventral and dorsal brain surface is proportional to influx into the brain parenchyma.

Because duration under anesthesia may alter how much CSF can move into the brain parenchyma, we anesthetized a group of animals with ISO for 2 hours before a standard CM injection of CSF tracer. We found that total tracer influx matched that in animals injected with CSF tracer within 15 min of anesthesia, indicating that long-term ISO anesthesia does not affect overall glymphatic function (fig. S4).

Delta band EEG power correlates strongly with glymphatic influx during anesthesia

We next asked whether neural activity patterns during anesthesia were proportional to glymphatic tracer influx. Previous work from our laboratory has demonstrated that fluid movement along the

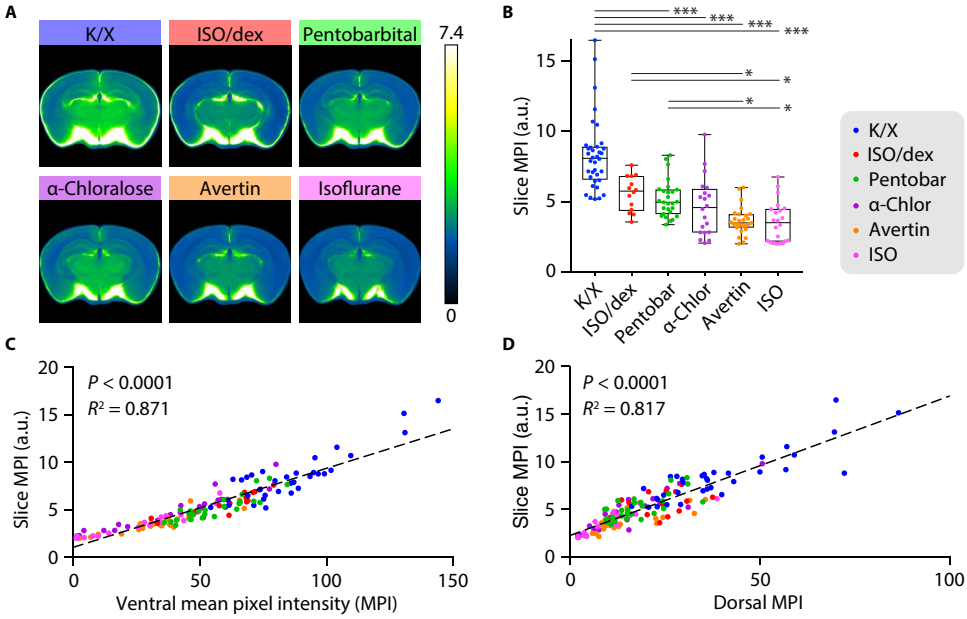

Fig. 2. Anesthetic agents differentially alter CSF tracer distribution in coronal brain sections. (**A**) Population-based median tracer distribution within the most posterior slice position in the six groups of anesthetized mice. (**B**) Boxplot displaying average tracer distribution across all brain slices (each dot represents the average of one brain) in the six groups of anesthetized mice (whiskers, minimum and maximum; box, quartiles; and line, median). Kruskal-Wallis test followed by Bonferroni correction, **P* < 0.05, ****P* < 0.001. (**C** and **D**) Correlation between CSF tracer distribution in coronal slices (slice MPI) and tracer distribution at the (C) ventral and (D) dorsal surfaces. K/X, *n* = 36 animals; ISO supplemented with dex, *n* = 14 animals; pentobarbital, *n* = 27 animals; α-chloralose, *n* = 20 animals; tribromoethanol, *n* = 27 animals; and ISO, *n* = 22 animals.

perivascular space is increased during sleep and K/X anesthesia (*5*). We propose that this could be a consequence of the high prevalence of delta band power or slow 1 to 4 Hz oscillations of highly synchronized neuronal activity in those conditions. To test this relationship, we measured EEG activity under the six different anesthesia regimens in a separate cohort of mice (Fig. 3 and fig. S5). Power spectrum analysis of the EEG recordings showed that K/X-anesthetized mice exhibited the highest power of delta wave oscillations (Fig. 3, A and B, and fig. S5A). Mice under ISO anesthesia supplemented with dex had significantly higher percent prevalence of delta power compared to the mice administered ISO alone (for exact *P* values, see table S1). There was no significant difference between the ISO and ISO supplemented with dex groups for any other frequency band of the EEG. Mice treated with other anesthetics showed intermediate percent prevalence of delta band power.

To determine whether tracer influx had an overall correlation with EEG, we conducted a linear regression analysis of tracer influx (slice MPIs) across all six anesthetic agents against EEG band powers. The prevalence of the delta band was highly predictive of the MPI across the six anesthetic groups (Fig. 3B). Of the EEG bands, beta power (13 to 20 Hz) had the highest correlation value but made up less than 10% of the overall EEG signal (Fig. 3C). Neither theta (4 to 8 Hz) nor alpha (8 to 13 Hz) power correlated significantly with slice MPIs across the entire group of mice (Fig. 3, D and E).

Heart rate is inversely related to glymphatic influx

Many factors can conceivably influence brain vasculature and perivascular fluid movement, including intracranial pressure, blood pressure, heart rate, and respiratory rate (*4*). However, we observed no significant difference in intracranial pressure between our anesthetic groups [analysis of variance (ANOVA) test, $F(5,27) = 0.4805$, $P = 0.7876$; fig. S6] and thus did not include intracranial pressure in our analyses. We then systematically measured blood pressure, heart rate, and respiratory rate under the different anesthesia conditions within the same animals from the EEG study (Fig. 4). Mice treated with K/X, the anesthetic combination associated with the greatest tracer influx, had the lowest mean heart rate (fig. S7 and table S1). The only outcome influenced by dex was heart rate, which exhibited a significant decrease compared to ISO alone. Pentobarbital, α-chloralose, ISO, and Avertin mouse groups all showed intermediate systolic blood pressure, heart rate, and respiratory rate. To better understand how these anesthetic-induced cardiopulmonary changes correlated to CSF tracer influx, we again performed a linear regression analysis between the group-wise means of slice MPIs and the various parameters. Of the three parameters, only heart rate had a significant (negative) correlation with tracer influx (Fig. 4).

DISCUSSION

In this study, we demonstrate that the choice of anesthetic agent can greatly influence CSF tracer influx. We probed the relationship between glymphatic influx with neuronal network activity (as measured by EEG) and cardiopulmonary parameters. Our analysis showed that the power of slow wave delta oscillations between 1 and 4 Hz was especially correlated to high influx of CSF tracers into the brain. Beta power also had some predictive value but accounted for less than 10% of the overall EEG signal. Neither alpha nor gamma wave powers correlated with glymphatic tracer influx. Heart rate under anesthesia exhibited a strong inverse relationship with glymphatic influx, whereas neither respiratory rate nor systolic blood pressure correlated to CSF tracer influx. ISO, Avertin, and α-chloralose anesthesia resulted in the lowest amount of fluorescent tracer uptake

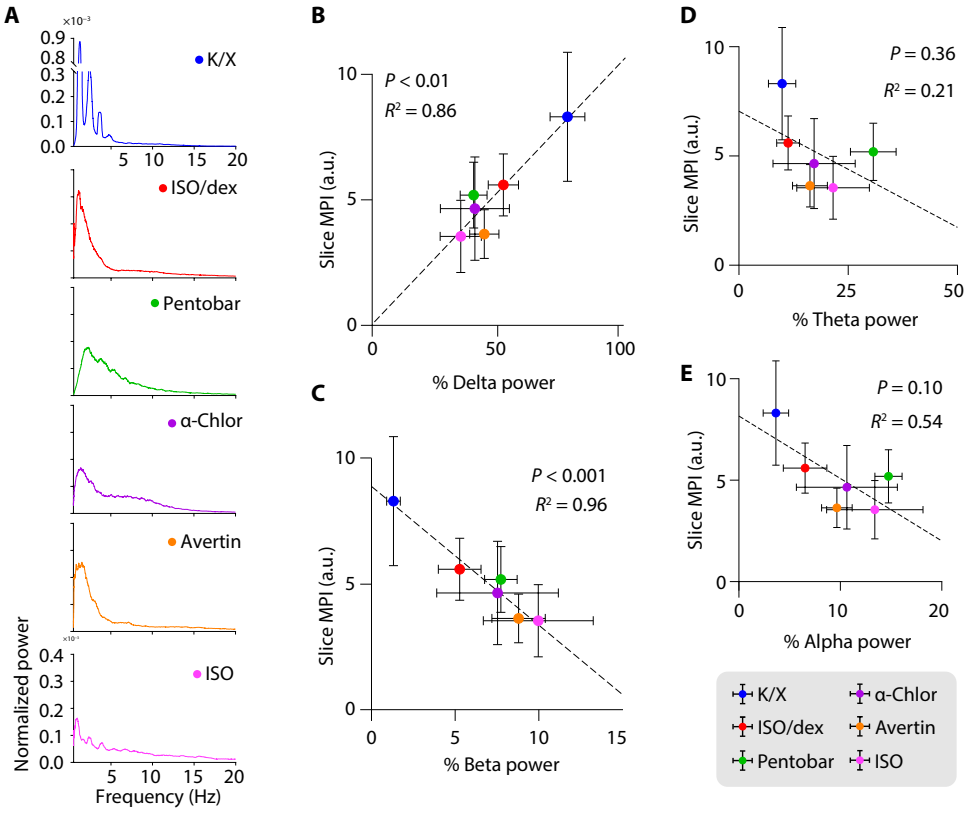

Fig. 3. Glymphatic tracer influx correlates with the prevalence of slow delta waves. (**A**) Representative normalized EEG power spectra for each anesthetic regimen. (**B** to **E**) Scatterplots depicting the correlation between MPI in coronal slices and the prevalence of delta (B), beta (C), theta (D), and alpha (E) EEG band power. Each dot represents the group mean (whiskers, SD). Correlations were calculated using group means; *P* values and R^2 values are displayed for each correlation. K/X, *n* = 36 animals for influx and 8 animals for EEG; ISO supplemented with dex, *n* = 14 animals for influx and 7 animals for EEG; pentobarbital, *n* = 27 animals for influx and 8 animals for EEG; α-chloralose, *n* = 20 animals for influx and 8 animals for EEG; tribromoethanol, *n* = 27 animals for influx and 5 animals for EEG; and ISO, *n* = 23 animals for influx and 6 animals for EEG.

in the brain, whereas mice anesthetized with pentobarbital anesthesia showed intermediate tracer influx. Consistent with previous work (*7*), the suppression of glymphatic activity by ISO was partially counteracted by supplementation with the α_2 agonist dex, while influx was highest in the K/X anesthesia group. These findings were seen consistently in the dorsal and ventral brain and throughout coronal sections of the brain. We conclude that K/X is the preferred agent among those tested here for mouse studies of CSF movement into and through the brain parenchyma.

The glymphatic model of bulk flow of fluid through the perivascular spaces in the brain has recently evoked controversies (*8*, *15*–*17*). The publications disputing the original findings have in common their use of multiple different types of anesthetics. For example, one paper challenging the glymphatic model uses Avertin (*8*), which we here show to be a poor choice of anesthetic for promoting tracer influx. In another study entailing CM tracer injections under ISO anesthesia, tracer distribution decreased with increased ISO concentration. That same study reported no increased influx under K/X anesthesia compared to awake animals, yet the initial infusion of tracer was performed under ISO, essentially mixing anesthetics in the experimental design (*17*). While it is unclear why these different compounds, with different mechanisms of action, enable or impair fluid movement within brain tissue, careful selection of an anesthetic agent emerges as a key factor in the novel biological system of glymphatic fluid transport.

The glymphatic system is regulated by the sleep-wake cycle, and we show that increased delta band power and decreased heart rate are correlated to improved glymphatic flow. In instances of sleep disruption, such as insomnia, the prevalence of the delta band in the first non-rapid eye movement (NREM) sleep of the night diminishes while the heart rate variability increases (*18*–*20*). Conversely, sleep occurring after prolonged sleep deprivation has higher incidence of delta power (*21*), and heart rate variability can be used as an accurate measure of EEG-scored vigilance state during sleep deprivation (*22*). By understanding the interplay between these three adjacent systems—neuronal circuitry, glymphatic fluid movement, and vasculature—we can better understand homeostatic processes such as sleep and arousal. One important observation that can be drawn from our study is that the pharmacodynamics mechanism of anesthetic-induced unconsciousness, i.e., *N*-methyl-D-aspartate receptor (NMDAR) antagonism or allosteric modulation of $GABA_A$ receptors, appears to be less important for glymphatic function than the effect of the anesthetics on slow delta wave or heart rate.

Of the six anesthetic agents tested here, ISO and dex are widely used in the clinic. Our analysis showed that anesthesia with ISO alone impedes glymphatic function, while dex has the opposite effect. These observations may provide insight into the known clinical effects of ISO and dex. Long-term sedation in intensive care units and general anesthesia for surgery are associated with cognitive disturbances, especially

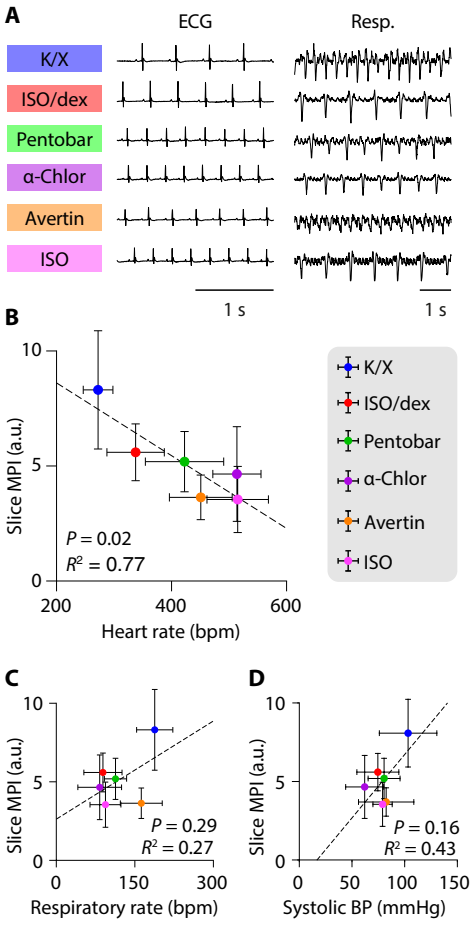

Fig. 4. Glymphatic tracer influx is inversely correlated with heart rate. (**A**) Representative traces of electrocardiogram and respiratory measurements for the six anesthetic regimens. (**B** to **D**) Scatterplots showing the correlation between MPI in coronal slices and heart rate (B), respiratory rate (C), and systolic blood pressure (BP) (D) across all anesthetic groups. Each dot represents the group mean (whiskers, SD). Correlations were calculated using group means; *P* values and R^2 values are displayed for each correlation. K/X, *n* = 36 animals for influx and 9 animals for cardiopulmonary measurements; ISO supplemented with dex, *n* = 14 animals for influx and 7 animals for cardiopulmonary measurements (CPMs); pentobarbital, n = 27 animals for influx and 8 animals for CPMs; tribromoethanol, *n* = 27 animals for influx and 5 animals for CPMs; α-chloralose, *n* = 20 animals for influx and 8 animals for CPMs; and ISO, *n* = 23 animals for influx and 7 animals for CPMs.

Table 1. Drug mechanism(s) of action. This table provides a summary of how different drugs used in this study modulate neurotransmission. The drug name is listed on the left, potential targets of each drug are listed in the middle, and references for more in-depth descriptions are provided on the right. NMDAR, *N*-methyl-D-aspartate receptor; 5-HT, 5-hydroxytryptamine; K_{2P}, two-pore potassium; HCN, hyperpolarization-activated cyclic nucleotide-gated.

Drug	Mechanism of action	References
Ketamine	NMDAR antagonist	(*32*, *33*)
Xylazine	α_2-Adrenergic receptor agonist	(*32*, *34*, *35*)
Pentobarbital	Positive allosteric modulator of $GABA_A$ chloride channels	(*32*, *36*)
α-Chloralose	Positive allosteric modulator of $GABA_A$ chloride channels	(*32*, *37*, *38*)
Avertin(2,2,2-tribromoethanol)	Unclear. Potential: agonist for $GABA_A$ and glycine receptors, negative allosteric modulator for dopaminergic, 5-HT, opioid, muscarinic, and adrenergic receptors	(*32*, *37*)
Isoflurane	Positive allosteric modulator of $GABA_A$ chloride channels; NMDAR, K_{2P} channel, and HCN channel antagonist	(*37*, *39*, *40*)
Dexmedetomidine	More potent and more selective α_2-adrenergic receptor agonist than xylazine	(*32*, *35*)

in the elderly population (*23*). Patients receiving inhalation anesthetics exhibit a high rate of delirium upon emergence from anesthesia (*24*). Conversely, prophylactic dex decreased the incidence of delirium in the postoperative setting compared with placebo (*25*). Several randomized controlled trials have demonstrated the superiority of dex to $GABA_A$ agonists, specifically benzodiazepines and propofol, in maintaining cognitive performance in intensive care patients (*26*–*28*). This clinical finding fits well with our results that dex and xylazine both enhance CSF influx into the brain, while ISO reduces glymphatic function. Although the involvement of the glymphatic system in cognitive performance and delirium remains to be established, it is compelling to hypothesize that promoting CSF delivery to the brain and improving clearance of metabolic waste present a mechanism explaining why dex decreases the incidence, while inhalation anesthesia increases the incidence of delirium. Previous preclinical studies have shown that inhalation anesthetics increase β amyloid accumulation in vivo (*29*) and promote its oligomerization in vitro (*30*). Both findings are consistent with a detrimental effect of ISO anesthesia on both glymphatic flow and neurotoxic effects of β amyloid.

In conclusion, we have demonstrated that the proper choice of an anesthetic, one which increases delta power and reduces heart rates, is essential for optimizing glymphatic function in preclinical rodent studies. Moreover, understanding ways to support proper perivascular fluid flow may prove crucial for rapid cognitive recovery following anesthesia in the clinic.

MATERIALS AND METHODS

Animals

Male and female C57BL/6 mice (ages 3 to 5 months and weight between 25 and 30 g) were acquired from Charles River Laboratories (Wilmington, MA, USA) in equal numbers for each experimental group to control for any potential sex differences. Mice were group-housed in a 12-hour light/12-hour dark cycle with ad libitum access to food and water. All experiments were performed in the light phase of the light/dark cycle. All experiments were approved by the University of Rochester Medical

Center Committee on Animal Resources. All efforts were made to keep animal usage to a minimum.

Drugs

Anesthesia was administered as follows: a mixture of racemic ketamine (100 mg/kg) and xylazine (20 mg/kg) intraperitoneally (ip), pentobarbital (60 mg/kg ip), 2,2,2-tribromoethanol (also known as Avertin; 120 mg/kg ip), α-chloralose (80 mg/kg ip), and ISO (initial induction at 4%, maintained at 1 to 2% for the duration of the experiment). For the α-chloralose regimen, surgery was initially done under 1 to 2% ISO and maintained at 0.5% ISO following CM injection because the drug is technically a hypnotic rather than a general anesthetic. In a separate cohort of mice, dex was given as a supplement to ISO induction at 0.015 mg/kg ip, with a second equal-sized bolus administered just before the 30-min tracer circulation period. ISO was always delivered with 100% oxygen. Depth of anesthesia was determined by the pedal reflex test. If the mouse responded to toe pinch an additional $^{1}/_{10}$ of the initial dosage was given and the tracer experiment was delayed until full unconsciousness was obtained. Directly before CM infusion, the animal received an additional $^{1}/_{10}$ of the initial dosage, and the pedal reflex was tested every 5 to 10 min during the tracer circulation time to ensure proper anesthesia throughout the study. Animals under Avertin anesthesia were most likely to need supplemental dosing. For mechanisms of action of each drug, please see Table 1.

Intracisternal CSF tracer infusion

The fluorescent CSF tracer (bovine serum albumin, Alexa Fluor 647 conjugate, Invitrogen, Life Technologies, Eugene, OR, USA; 66 kDa) was formulated in artificial CSF at a concentration of 0.5% (w/v). Anesthetized mice were fixed in a stereotaxic frame, the CM was surgically exposed, and a 30-gauge needle connected to PE10 tubing filled with the tracer was inserted into the CM. Ten microliters of CSF tracer was infused at a rate of 2 μl/min for 5 min with a syringe pump (Harvard Apparatus) (*31*). All experiments were done by the same operator, in a semi-interleaved fashion. Group data were repeated over at least two experimental days to ensure reproducibility. To visualize tracer movement from the cisternal compartments into the brain parenchyma, the animals were euthanized by decapitation and the brain was removed 30 min after the start of intracisternal infusion (note that the needle was left in place after the infusion). The brain was fixed overnight by immersion in 4% paraformaldehyde in phosphate-buffered saline. Coronal vibratome slices (100 μm) were cut and mounted. Tracer influx into the brain was imaged ex vivo by macroscopic whole-brain and whole-slice conventional fluorescence microscopy (Olympus; Stereo Investigator Software).

Tracer influx was quantified independently by two sets of blinded investigators using FIJI (ImageJ) software, as described previously (*1*). Each coronal slice was manually outlined, and the mean fluorescence intensity within the ROIs was measured. Average fluorescence intensity was calculated across six slices for a single animal, resulting in a single biological replicate. Equivalent slices were used for all biological replicates.

Population-based average intensity image generation

To allow qualitative visual comparison of the effects of individual anesthetics on CSF tracer influx, a population-based average combining the images from all anesthesia groups was created for each of the image types: ventral and dorsal macroscopic images (Fig. 1) and coronal slices (Fig. 2 and fig. S3). First, an initial average template was computed as the mean of the nonaligned images. Then, all images were registered to this average template, and a new mean of the aligned images was computed. Registering and averaging were repeated with increasingly refined registration methods (four iterations of rigid registration, followed by two affine registration iterations and lastly by four nonlinear registration iterations), resulting in the final population-based average template. Last, all images were nonlinearly registered to the appropriate template to allow group comparisons. Image registration was performed using Advanced Normalization Tools (ANTs) 2.1.0 and scripted with Python 3.6.

EEG and cardiovascular outcomes experiment

EEG recordings were obtained by commercial telemetric electrodes (Pinnacle Technology). The head plate was mounted under 2% ISO anesthesia, and small burr holes were drilled in the skull 2.5 mm lateral and 2 mm posterior to the bregma on either side of the midline. EEG wire leads were then inserted into the burr holes on one side of the midline between the skull and underlying dura. EEG leads were secured to the skull with dental acrylic. An electromyogram (EMG) lead was inserted in the neck muscle. The animals recovered for 7 days before EEG and EMG measurements were made.

A week after implantation and recovery, animals were anesthetized, as above. The EEG and EMG signal was then recorded for 10 min along with 10-min sessions in a blood pressure tail cuff to measure systolic blood pressure, heart rate, and respiratory rate recording for 5 min. The type of anesthesia was randomized throughout the experiment, with each animal receiving a new anesthetic every 3 days, thus reducing drug-ordering effect and giving the animal sufficient time to recover from deep anesthesia.

Anesthetized mice were placed on a thermostatic pad during EEG and EMG recording sessions. Signals were collected with Clampex 10.2 (sampling rate, 1000 Hz). EEG data were analyzed using a customized MATLAB script. The Chronux toolbox (http://chronux.org/) was used to calculate relative and absolute power of each band (delta, 1 to 4 Hz; theta, 4 to 8 Hz; alpha, 8 to 13 Hz; and beta, 13 to 20 Hz).

Heart rate, blood pressure, and respiratory rate were monitored via the Small Animal Physiological Monitoring System (Harvard Apparatus, Holliston, MA, USA). Here, heart rate and respiratory rate were reported as averages across 5 min of monitoring while under anesthesia. Blood pressure was monitored noninvasively by tail cuff with the CODA high-throughput system (Kent Scientific).

Intracranial pressure measurement

Intracranial pressure was measured through a catheter placed in the CM and connected to a pressure transducer and monitor (World Precision Instruments). The signals were digitized and recorded with a Digidata 1550A digitizer and AxoScope software (Axon Instruments).

Statistical analysis

Data are presented as means ± SD, unless otherwise noted. All statistical analysis was performed in Python 3.6, MATLAB 9.3, or GraphPad Prism 7.0d. For comparisons of means in samples with normal distributions and homogeneous variances (as indicated by a Levene's test), ANOVA was used for comparisons between two or more means, followed by Bonferroni *P* value correction for multiple comparisons. In cases of a non-normal distribution (as indicated by a Shapiro Wilk test) or unequal variances (Levene's test), a nonparametric Kruskal-Wallis test was used for comparisons between two or more means,

followed by Bonferroni P value correction for multiple comparisons. Linear least squares regression was used for calculation of correlations between group averages of EEG band powers, cardiovascular measures, and tracer MPIs. Significance was ascribed at $P < 0.05$.

SUPPLEMENTARY MATERIALS

Supplementary material for this article is available at http://advances.sciencemag.org/cgi/content/full/5/2/eaav5447/DC1

Fig. S1. Index of sections from each anesthetic group.
Fig. S2. Subregion analysis of glymphatic influx in coronal slices.
Fig. S3. Analysis of interior brain slices under anesthesia.
Fig. S4. Two hours of ISO do not improve glymphatic influx.
Fig. S5. Comparisons of EEG power spectrum prevalence across anesthetic regimens.
Fig. S6. Comparison of intracranial pressure across anesthetic regimens.
Fig. S7. Comparisons of cardiovascular measurements across anesthetic regimens.
Table S1. Statistical comparison of parameters between anesthetic regimens.

REFERENCES AND NOTES

1. J. J. Iliff, M. Wang, Y. Liao, B. A. Plogg, W. Peng, G. A. Gundersen, H. Benveniste, G. E. Vates, R. Deane, S. A. Goldman, E. A. Nagelhus, M. Nedergaard, A paravascular pathway facilitates CSF flow through the brain parenchyma and the clearance of interstitial solutes, including amyloid β. *Sci. Transl. Med.* **4**, 147ra111 (2012).
2. N. A. Jessen, A. S. Munk, I. Lundgaard, M. Nedergaard, The glymphatic system: A beginner's guide. *Neurochem. Res.* **40**, 2583–2599 (2015).
3. H. Mestre, L. M. Hablitz, A. L. R. Xavier, W. Feng, W. Zou, T. Pu, H. Monai, G. Murlidharan, R. M. Castellanos Rivera, M. J. Simon, M. M. Pike, V. Plá, T. Du, B. T. Kress, X. Wang, B. A. Plog, A. S. Thrane, I. Lundgaard, Y. Abe, M. Yasui, J. H. Thomas, M. Xiao, H. Hirase, A. Asokan, J. J. Iliff, M. Nedergaard, Aquaporin-4-dependent glymphatic solute transport in the rodent brain. *eLife* **7**, e40070 (2018).
4. B. A. Plog, M. Nedergaard, The glymphatic system in central nervous system health and disease: Past, present, and future. *Annu. Rev. Pathol.* **13**, 379–394 (2018).
5. L. Xie, H. Kang, Q. Xu, M. J. Chen, Y. Liao, M. Thiyagarajan, J. O'Donnell, D. J. Christensen, C. Nicholson, J. J. Iliff, T. Takano, R. Deane, M. Nedergaard, Sleep drives metabolite clearance from the adult brain. *Science* **342**, 373–377 (2013).
6. M. DiNuzzo, M. Nedergaard, Brain energetics during the sleep-wake cycle. *Curr. Opin. Neurobiol.* **47**, 65–72 (2017).
7. H. Benveniste, H. Lee, F. Ding, Q. Sun, E. al-Bizri, R. Makaryus, S. Probst, M. Nedergaard, E. A. Stein, H. Lu, Anesthesia with dexmedetomidine and low-dose isoflurane increases solute transport *via* the glymphatic pathway in rat brain when compared with high-dose isoflurane. *Anesthesiology* **127**, 976–988 (2017).
8. A. J. Smith, X. Yao, J. A. Dix, B.-J. Jin, A. S. Verkman, Test of the "glymphatic" hypothesis demonstrates diffusive and aquaporin-4-independent solute transport in rodent brain parenchyma. *eLife* **6**, e27679 (2017).
9. H. Mestre, S. Kostrikov, R. I. Mehta, M. Nedergaard, Perivascular spaces, glymphatic dysfunction, and small vessel disease. *Clin. Sci.* **131**, 2257–2274 (2017).
10. A. V. Rodriguez, C. M. Funk, V. V. Vyazovskiy, Y. Nir, G. Tononi, C. Cirelli, Why does sleep slow-wave activity increase after extended wake? Assessing the effects of increased cortical firing during wake and sleep. *J. Neurosci.* **36**, 12436–12447 (2016).
11. L. de Vivo, M. Bellesi, W. Marshall, E. A. Bushong, M. H. Ellisman, G. Tononi, C. Cirelli, Ultrastructural evidence for synaptic scaling across the wake/sleep cycle. *Science* **355**, 507–510 (2017).
12. B. Musizza, A. Stefanovska, P. V. E. McClintock, M. Paluš, J. Petrovčič, S. Ribarič, F. F. Bajrović, Interactions between cardiac, respiratory and EEG-delta oscillations in rats during anaesthesia. *J. Physiol.* **580**, 315–326 (2007).
13. J. J. Iliff, M. Wang, D. M. Zeppenfeld, A. Venkataraman, B. A. Plog, Y. Liao, R. Deane, M. Nedergaard, Cerebral arterial pulsation drives paravascular CSF-interstitial fluid exchange in the murine brain. *J. Neurosci.* **33**, 18190–18199 (2013).
14. B. Bedussi, D. M. P. Naessens, J. de Vos, R. Olde Engberink, M. M. M. Wilhelmus, E. Richard, M. ten Hove, E. vanBavel, E. N. T. P. Bakker, Enhanced interstitial fluid drainage in the hippocampus of spontaneously hypertensive rats. *Sci. Rep.* **7**, 744 (2017).
15. N. J. Abbott, M. E. Pizzo, J. E. Preston, D. Janigro, R. G. Thorne, The role of brain barriers in fluid movement in the CNS: Is there a "glymphatic" system? *Acta Neuropathol.* **135**, 387–407 (2018).
16. A. J. Smith, A. S. Verkman, The "glymphatic" mechanism for solute clearance in Alzheimer's disease: Game changer or unproven speculation? *FASEB J.* **32**, 543–551 (2018).
17. C. Gakuba, T. Gaberel, S. Goursaud, J. Bourges, C. di Palma, A. Quenault, S. M. de Lizarrondo, D. Vivien, M. Gauberti, General anesthesia inhibits the activity of the "glymphatic system". *Theranostics* **8**, 710–722 (2018).
18. F. Jurysta, J. P. Lanquart, V. Sputaels, M. Dumont, P. F. Migeotte, S. Leistedt, P. Linkowski, P. van de Borne, The impact of chronic primary insomnia on the heart rate–EEG variability link. *Clin. Neurophysiol.* **120**, 1054–1060 (2009).
19. S. D. Rothenberger, R. T. Krafty, B. J. Taylor, M. R. Cribbet, J. F. Thayer, D. J. Buysse, H. M. Kravitz, E. D. Buysse, M. H. Hall, Time-varying correlations between delta EEG power and heart rate variability in midlife women: The SWAN Sleep Study. *Psychophysiology* **52**, 572–584 (2015).
20. V. Svetnik, E. S. Snyder, J. Ma, P. Tao, C. Lines, W. J. Herring, EEG spectral analysis of NREM sleep in a large sample of patients with insomnia and good sleepers: Effects of age, sex and part of the night. *J. Sleep Res.* **26**, 92–104 (2017).
21. E. Olbrich, H. P. Landolt, P. Achermann, Effect of prolonged wakefulness on electroencephalographic oscillatory activity during sleep. *J. Sleep Res.* **23**, 253–260 (2014).
22. E. C.-P. Chua, W.-Q. Tan, S.-C. Yeo, P. Lau, I. Lee, I. H. Mien, K. Puvanendran, J. J. Gooley, Heart rate variability can be used to estimate sleepiness-related decrements in psychomotor vigilance during total sleep deprivation. *Sleep* **35**, 325–334 (2012).
23. S. Paredes, L. Cortínez, V. Contreras, B. Silbert, Post-operative cognitive dysfunction at 3 months in adults after non-cardiac surgery: A qualitative systematic review. *Acta Anaesthesiol. Scand.* **60**, 1043–1058 (2016).
24. J. D. Brioni, S. Varughese, R. Ahmed, B. Bein, A clinical review of inhalation anesthesia with sevoflurane: From early research to emerging topics. *J. Anesth.* **31**, 764–778 (2017).
25. X. Su, Z. T. Meng, X. H. Wu, F. Cui, H. L. Li, D. X. Wang, X. Zhu, S. N. Zhu, M. Maze, D. Ma, Dexmedetomidine for prevention of delirium in elderly patients after non-cardiac surgery: A randomised, double-blind, placebo-controlled trial. *Lancet* **388**, 1893–1902 (2016).
26. S. M. Jakob, E. Ruokonen, R. M. Grounds, T. Sarapohja, C. Garratt, S. J. Pocock, J. R. Bratty, J. Takala; Dexmedetomidine for Long-Term Sedation Investigators, Dexmedetomidine vs midazolam or propofol for sedation during prolonged mechanical ventilation: Two randomized controlled trials. *JAMA* **307**, 1151–1160 (2012).
27. P. P. Pandharipande, B. T. Pun, D. L. Herr, M. Maze, T. D. Girard, R. R. Miller, A. K. Shintani, J. L. Thompson, J. C. Jackson, S. A. Deppen, R. A. Stiles, R. S. Dittus, G. R. Bernard, E. W. Ely, Effect of sedation with dexmedetomidine vs lorazepam on acute brain dysfunction in mechanically ventilated patients: The MENDS randomized controlled trial. *JAMA* **298**, 2644–2653 (2007).
28. R. R. Riker, Y. Shehabi, P. M. Bokesch, D. Ceraso, W. Wisemandle, F. Koura, P. Whitten, B. D. Margolis, D. W. Byrne, E. W. Ely, M. G. Rocha; SEDCOM (Safety and Efficacy of Dexmedetomidine Compared With Midazolam) Study Group, Dexmedetomidine vs midazolam for sedation of critically ill patients: A randomized trial. *JAMA* **301**, 489–499 (2009).
29. Z. Xie, D. J. Culley, Y. Dong, G. Zhang, B. Zhang, R. D. Moir, M. P. Frosch, G. Crosby, R. E. Tanzi, The common inhalation anesthetic isoflurane induces caspase activation and increases amyloid β-protein level in vivo. *Ann. Neurol.* **64**, 618–627 (2008).
30. R. G. Eckenhoff, J. S. Johansson, H. Wei, A. Carnini, B. Kang, W. Wei, R. Pidikiti, J. M. Keller, M. F. Eckenhoff, Inhaled anesthetic enhancement of amyloid-β oligomerization and cytotoxicity. *Anesthesiology* **101**, 703–709 (2004).
31. H. Mestre, J. Tithof, T. du, W. Song, W. Peng, A. M. Sweeney, G. Olveda, J. H. Thomas, M. Nedergaard, D. H. Kelley, Flow of cerebrospinal fluid is driven by arterial pulsations and is reduced in hypertension. *Nat. Commun.* **9**, 4878 (2018).
32. R. E. Meyer, R. E. Fish, Pharmacology of injectable anesthetics, sedatives and tranquilizers, in *Anesthesia and Analgesia in Laboratory Animals (Second Edition)*, R. E. Fish, M. J. Brown, P. J. Danneman, A. Z. Karas, Eds, (Academic Press, San Diego, 2008), pp. 27–82.
33. G. Mion, T. Villevieille, Ketamine pharmacology: An update (pharmacodynamics and molecular aspects, recent findings). *CNS Neurosci. Ther.* **19**, 370–380 (2013).
34. W. H. Hsu, Xylazine-induced depression and its antagonism by alpha adrenergic blocking agents. *J. Pharmacol. Exp. Ther.* **218**, 188–192 (1981).
35. J. W. Park, H. W. Chung, E. J. Lee, K.-H. Jung, J.-Y. Paik, K.-H. Lee, α2-Adrenergic agonists including xylazine and dexmedetomidine inhibit norepinephrine transporter function in SK-N-SH cells. *Neurosci. Lett.* **541**, 184–189 (2013).
36. M. Davies, R. P. Thuynsma, S. M. Dunn, Effects of propofol and pentobarbital on ligand binding to $GABA_A$ receptors suggest a similar mechanism of action. *Can. J. Physiol. Pharmacol.* **76**, 46–52 (1998).
37. M. D. Krasowski, N. L. Harrison, The actions of ether, alcohol and alkane general anaesthetics on $GABA_A$ and glycine receptors and the effects of TM2 and TM3 mutations. *Br. J. Pharmacol.* **129**, 731–743 (2000).
38. K. M. Garrett, J. Gan, Enhancement of γ-aminobutyric $acid_A$ receptor activity by α-chloralose. *J. Pharmacol. Exp. Ther.* **285**, 680–686 (1998).
39. D. B. Brunson, Chapter 3 - Pharmacology of inhalation anesthetics, in *Anesthesia and Analgesia in Laboratory Animals (Second Edition)*, R. E. Fish, M. J. Brown, P. J. Danneman, A. Z. Karas, Eds, (Academic Press, San Diego, 2008), pp. 83–95.

40. H. C. Hemmings Jr., M. H. Akabas, P. A. Goldstein, J. R. Trudell, B. A. Orser, N. L. Harrison, Emerging molecular mechanisms of general anesthetic action. *Trends Pharmacol. Sci.* **26**, 503–510 (2005).

Acknowledgments: We thank P. Cumming for comments on the manuscript and D. Xue for graphic illustrations and animations. **Funding:** This project has received funding from the NIH/NINDS/NIA, the Adelson Foundation, the Sigrid Juselius Foundation, the Novo Nordisk Foundation, the Lundbeck Foundation, JPND research, and DACAP-AD. **Author contributions:** L.M.H. and M.N. were responsible for experimental design. L.M.H., H.S.V., and Q.S. were responsible for data collection. L.M.H., H.S.V., Q.S., F.F.S., B.S., and K.N.M. were responsible for data analysis. L.M.H. and F.F.S. were responsible for figure preparation. L.M.H., T.O.L., and M.N. were responsible for manuscript writing and preparation. All authors have read and have approved the final version of this manuscript. **Competing interests:** The authors declare that they have no competing interests. **Data availability:** All data needed to evaluate the conclusions in the paper are present in the paper and/or the Supplementary Materials. Additional data related to this paper may be requested from the authors.

Submitted 27 September 2018
Accepted 14 January 2019
Published 27 February 2019
10.1126/sciadv.aav5447

Citation: L. M. Hablitz, H. S. Vinitsky, Q. Sun, F. F. Stæger, B. Sigurdsson, K. N. Mortensen, T. O. Lilius, M. Nedergaard, Increased glymphatic influx is correlated with high EEG delta power and low heart rate in mice under anesthesia. *Sci. Adv.* **5**, eaav5447 (2019).

ScienceAdvances

Increased glymphatic influx is correlated with high EEG delta power and low heart rate in mice under anesthesia

Lauren M. Hablitz, Hanna S. Vinitsky, Qian Sun, Frederik Filip Stæger, Björn Sigurdsson, Kristian N. Mortensen, Tuomas O. Lilius and Maiken Nedergaard

Sci Adv **5** (2), eaav5447.
DOI: 10.1126/sciadv.aav5447